Land Degradation & Development

WILEY

RESEARCH ARTICLE OPEN ACCESS

Carbon, Nitrogen, and Corresponding Stable Isotope Signatures Reveal Channel Banks as Major Sediment Sources in a Tropical Agricultural Watershed

Fábio Farias Amorim[1] | Yuri Jacques Agra Bezerra da Silva[2] | Rennan Cabral Nascimento[2] | Ygor Jacques Agra Bezerra da Silva[1] | Angelo Jamil Maia[1] | Tales Tiecher[3] | Jean Paolo Gomes Minella[4] | Yusheng Zhang[5] | Hari Ram Upadhayay[5] | Simon Pulley[5] | Adrian L. Collins[5]

[1]Department of Agronomy, Universidade Federal Rural de Pernambuco (UFRPE), Recife, Pernambuco, Brazil | [2]Department of Agricultural Engineering, Universidade Federal Rural de Pernambuco (UFRPE), Recife, Pernambuco, Brazil | [3]Department of Soil Science, Universidade Federal do Rio Grande do Sul (UFRGS), Interdisciplinary Research Group on Environmental Biogeochemistry (IRGEB), Porto Alegre, Rio Grande do Sul, Brazil | [4]Department of Soil Science, Universidade Federal de Santa Maria (UFSM), Santa Maria, Rio Grande do Sul, Brazil | [5]Rothamsted Research, North Wyke, Okehampton, UK

Correspondence: Yuri Jacques Agra Bezerra da Silva (yuri.silva@ufrpe.br)

Received: 25 June 2025 | **Revised:** 23 October 2025 | **Accepted:** 31 December 2025

Keywords: Bayesian modeling | catchment management | particle size | sediment fingerprinting | stable isotopes

ABSTRACT

Uncertainties about the applicability of $\delta^{13}C$ and $\delta^{15}N$ as tracers of sediment sources in tropical river basins highlight the need for more in-depth investigations of these isotopes. This study therefore assessed the effectiveness of $\delta^{13}C$ and $\delta^{15}N$ signatures in discriminating sediment sources in an agricultural catchment in Northeast Brazil. Three potential sediment sources were sampled as follows: unpaved roads, sugarcane cultivation, and channel banks. Suspended and riverbed sediments were used as target sediments. Source and sediment samples were sieved to two particle size fractions: <63 and $<32\,\mu m$. The isotopes were evaluated using conservativeness tests, Kruskal–Wallis, linear discriminant analysis, and virtual mixtures. Our results indicated that $\delta^{13}C$ and $\delta^{15}N$ together are effective tracers for modeling sediment sources, providing significant detail on sediment delivery patterns in a tropical catchment under intensive land use. Both fractions showed no significant differences in conservativeness or source apportionment. However, the $<63\,\mu m$ fraction yielded more robust discrimination potential and model estimates. Therefore, future studies in other catchments under similar conditions could focus on a single fraction, preferably the fraction $<63\,\mu m$, optimizing effort without compromising scientific robustness. Channel banks contributed the majority of sediment in both size fractions, indicating that agricultural expansion into riparian zones—resulting in the absence or inadequate type of vegetation cover—has accelerated erosion. This underscores the urgent need to restore riparian forests and protect these vulnerable areas, while also emphasizing the importance of developing innovative, interdisciplinary approaches to effectively manage and integrate riparian vegetation into landscape planning and water resource strategies.

1 | Introduction

Soil loss is one of the biggest threats to food security and environmental quality (Montanarella et al. 2016; Kopittke et al. 2019) since it decreases agricultural productivity and degrades water resources. This environmental threat is mainly driven by water erosion (Guo et al. 2019), which results in the transfer of sediment from soil to aquatic systems, redistribution on hillslopes, and deposition on the pediments and floodplains. Redistribution also plays a key role in transferring sediment-bound chemicals, including heavy metals. These contaminants are typically associated with smaller, less dense particulate

fractions such as clay, silt, microaggregates, and organic matter. Redistribution and delivery occur through surface (Dąbrowska et al. 2018) and subsurface runoff (Deasy et al. 2009), which are primarily controlled by rainfall characteristics, slope, soil properties, and land cover (Huang et al. 2020; Puntenney-Desmond et al. 2020). In the management of large river basins, diffuse sediment pollution makes it difficult to allocate resources for the effective control of erosion processes. Suspended sediment loads originate from multiple potential sources, and their contributions vary spatially and temporally (Haddadchi et al. 2013). Here, the robust discrimination of contributing areas within a catchment is a prerequisite for targeting mitigation (Collins and Walling 2004).

The methods for generating reliable information on sediment sources in catchments have been improved over recent decades and include visual observations, long-duration field surveys and the source fingerprinting approach (Reid and Dunne 1996; Gellis et al. 2005; Collins et al. 2017). Sediment fingerprinting involves employing tracers to identify the contributions from classified sources in a given catchment. This tracing technique uses a combination of field data collection, laboratory analyses of source material and target sediment samples, statistical analyses and numerical modeling (Davis and Fox 2009). The tracers that can be used in sediment fingerprinting may include geochemical signatures (Bahadori et al. 2019), weathering indices (Nosrati et al. 2019), radionuclides (Gellis et al. 2019), magnetic susceptibility (Rowntree et al. 2017), optical properties (Amorim et al. 2021), environmental DNA (Evrard et al. 2019), color properties from reflectance spectra (Liu et al. 2017), and others.

Although the fingerprinting approach is the currently recommended technique for sediment source apportionment, there are still uncertainties associated with this option (Mukundan et al. 2012), mainly in regard to sediment sorting (Gaspar et al. 2022) and tracer conservation and corresponding corrections in source apportionment modeling (Smith and Blake 2014), as well as catchment source classification (Pulley et al. 2017). In addition, the effectiveness of source fingerprinting requires distinctive tracer signatures between individual sediment sources. To overcome such limitations, composite signatures comprised of two or more properties are recommended (Collins et al. 2019). Models can be constructed using various combinations of parameters, including tracers, source group classifications, and particle size fractions. Notably, the reliability of source apportionment estimates can be assessed using virtual mixtures and evaluation metrics for accuracy and precision, leading to a more robust interpretation of source contributions (Collins et al. 2020; Batista et al. 2022).

Stable isotopes of C and N associated with soil and sediment organic matter have the potential to distinguish erosion processes linked to land use and occupation, aiding sediment source identification (Riddle et al. 2022; Abbas et al. 2024; Skadell et al. 2025). This is essential for reducing uncertainties in source fingerprinting modeling (Upadhayay et al. 2017). C and N are highly concentrated in the surface of agricultural soils but are typically lower in the deeper layers, such as in channel banks (Papanicolaou et al. 2003). Also, C and N stable isotope ratios ($\delta^{13}C$ and $\delta^{15}N$, respectively) are assumed to be well preserved in support of sediment source apportionment (Papanicolaou et al. 2003; Stewart et al. 2015), and are usually linked to the specific characteristics of the culture (Biggs et al. 2002).

The primary challenge in using C and N isotopes lies in the potential nonstationarity and lack of conservation of sediment isotopic signatures during transport and intermittent deposition within river channel systems (Fox and Martin 2015; Lizaga et al. 2022; Riddle et al. 2025). Organic matter in sediments can be oxidized and mineralized by microorganisms, altering $\delta^{13}C$ and $\delta^{15}N$ values. The accumulation of algae, which assimilate carbon and nitrogen with their own isotopic signatures, can also mask original values when they decompose and become incorporated into the sediment. Additionally, wastewater discharge may further modify these isotopic ratios.

Agricultural catchments under monoculture systems tend to exhibit soils with more homogeneous C and N isotopic signatures, which help attenuate the effects of nonstationarity in isotopic tracers within these soils (Leite et al. 2025; Skadell et al. 2025). In contrast, catchments with a greater diversity of crops produce more heterogeneous signatures. However, uncertainties remain concerning the variability of $\delta^{13}C$ and $\delta^{15}N$ and their potential use for source fingerprinting in catchments situated in tropical environments (Collins et al. 2019; Riddle et al. 2022), highlighting the necessity for further exploration of these specific tracers. Tropical environments, characterized by high flooding frequencies, can attenuate variations in isotopic signatures due to the rapid sediment delivery and transport processes. Under these conditions, even if only one isotopic tracer is validated in conservation tests, effective differentiation of sediment sources can still be achieved, owing to the successful application of stable isotopic tracers and their high discriminatory power between sources. Thus, this study assessed the effectiveness of isotopic signatures ($\delta^{13}C$ and $\delta^{15}N$) in discriminating and apportioning sediment sources in a tropical agricultural watershed in Northeastern Brazil.

2 | Material and Methods

2.1 | Study Catchment

The Tracunhaém catchment covers an area of ~1350 km^2 and is located in the northeastern region of Brazil (Figure 1). The area has a humid tropical climate, with rainfall predominantly occurring between April and August, ranging from 1150 to 2350 mm (west to east) annually (Santos et al. 2009). Average temperatures in the catchment range from 25°C to 27°C. The dominant parent materials include orthogneisses, calcsilicate rocks, and biotite gneisses (Figure 1), while Acrisols are the dominant soil type (IUSS Working Group WRB 2006). The relief is generally gentle, becoming moderately undulating in some areas, with slopes ranging from 2% to 18%.

2.2 | Sampling of Sources and Target Sediment

The catchment was identified as having three potential sediment sources based on land use and occupation: (i) sugarcane croplands (SC); (ii) unpaved roads (UR), and (iii) channel banks (CB). The choice of sampling sites for individual sediment sources was based

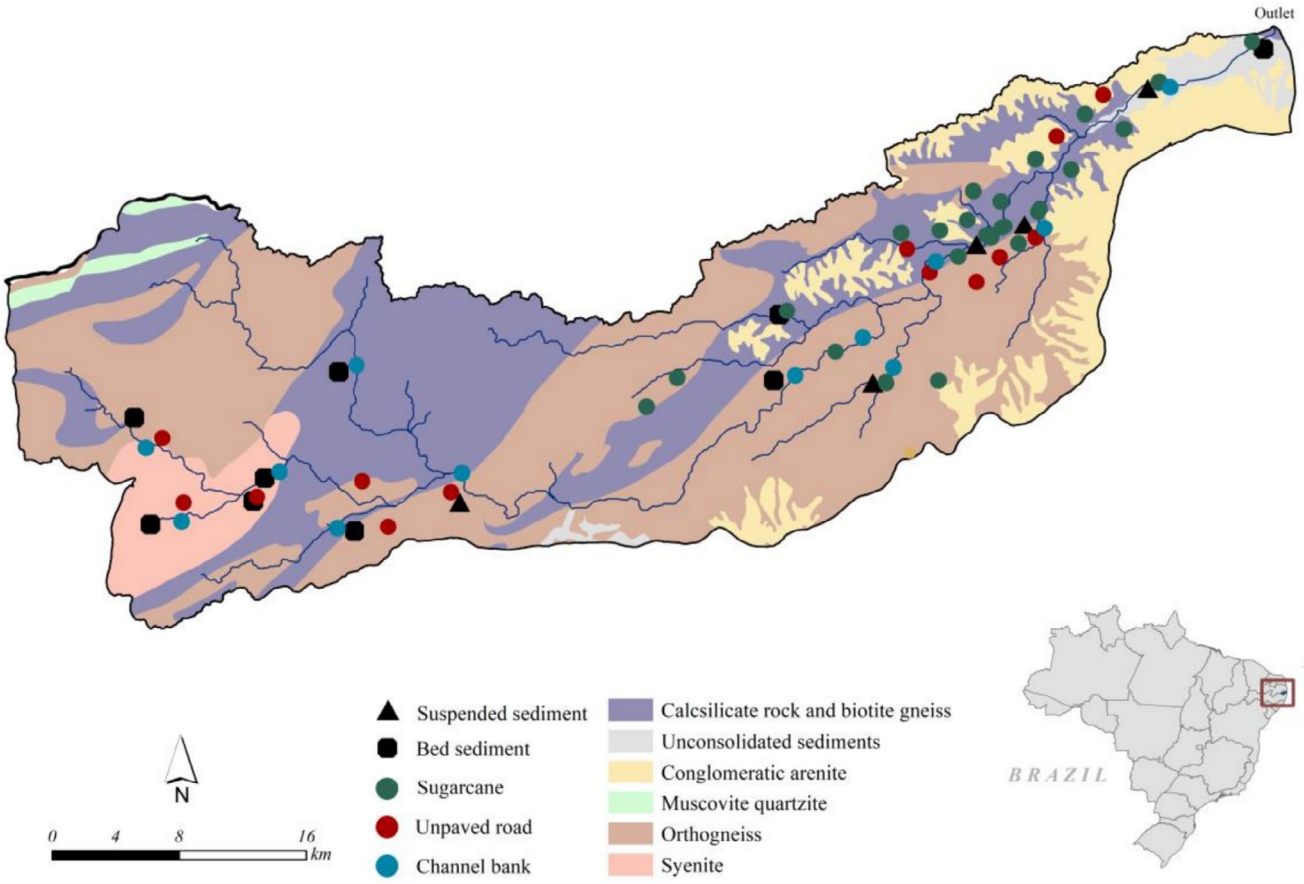

FIGURE 1 | Map of geological formations and the locations of sampling sites for potential sediment sources and target sediment samples within the Tracunhaém catchment, northeastern Brazil. [Colour figure can be viewed at wileyonlinelibrary.com]

on field observations, mainly assessing proximity to the river and evidence of erosion and sediment delivery pathways. A total of 51 composite samples were collected throughout the catchment: 26 from SC, 13 from UR, and 12 from eroding CB (Figure 1). Each sample was made up of 10 subsamples to represent the microspatial variability of the source properties (i.e., a total of 510 samples were collected). SC and UR samples were collected from the surface soil layer (0–5 cm), while CB samples encompassed the entire profile exposed to fluvial erosion. The overall number of samples took explicit consideration of the number of soil types and geological formations present in the study catchment.

Suspended sediment samples (SS; $n = 5$) distributed along the main watercourse, collected by time-integrated samplers (TIMS; Phillips et al. 2000), were used as one type of target sediment. Bed sediment (BS) composite samples ($n = 9$) were also collected with steel shovels. Each composite sample was made up of 10 subsamples to represent the spatial variability in the river cross-section. These bed sediment samples are representative of a single moment in time.

2.3 | Sample Preparation

The sediment samples were air-dried or dried in a forced-air oven at 50°C. They were then disaggregated and homogenized using a 2 mm sieve. Laser granulometry of the target sediments was conducted on 2 g aliquots, following oxidation of organic matter with 100–150 mL of 5% H_2O_2 and subsequent chemical dispersion using NaOH, as described by Muggler et al. (1997). The results indicated that the <63 and $<32\,\mu m$ fractions were the most suitable for tracer comparisons within the study basin (Figure 2). For SS, the $<63\,\mu m$ fraction accounted for 99%–100% of the samples, and the $<38\,\mu m$ fraction comprised approximately 89%–90%. In contrast, for BS, the $<63\,\mu m$ fraction represented 95%–96% of the samples, and the $<38\,\mu m$ fraction around 82%–83%.

Each sample was then split into two portions, with one fraction sieved through a $63\,\mu m$ stainless steel mesh and the other through a $32\,\mu m$ mesh; the most important sediment sizes exported by the main watercourse.

2.4 | Tracer Analyses

The total carbon (TC), total nitrogen (TN), $\delta^{13}C$, and $\delta^{15}N$ signatures were determined by an elemental analyzer (Carlo Erba NA2000) linked to a PDZ Europa 20–22 isotope ratio mass spectrometer. Wheat flour AI-R001 ($\delta^{13}C$ VPDE = −26.43‰, $\delta^{15}N$ AIR = +2.55‰, C = 40.2%, and $N = 1.88\%$) was the reference standard and calibrated with IAEA-N-1 (ammonium sulfate) for $^{15}N/^{14}N$ and IAEA-CH_6 (ANU Sucrose) for $^{12}C/^{13}C$ by Iso-Analytical. A wheat-flour-based quality control representing 10% of each analytical run was used to confirm the validity of the results. The atmospheric nitrogen was industry standard for $^{15}N/^{14}N$ (Mariotti 1983), while the Vienna-Pee Dee Belemnite

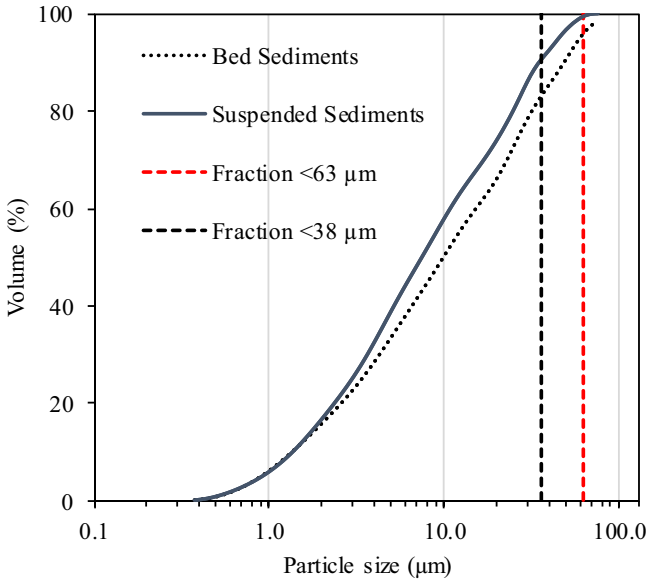

FIGURE 2 | Average cumulative absolute (i.e., chemically dispersed) particle size distributions of bed ($n = 4$) and suspended ($n = 4$) target sediment samples. [Colour figure can be viewed at wileyonlinelibrary.com]

Limestone was for $^{12}C/^{13}C$ (Bender 1971; Dalzell et al. 2007). The data are presented as natural abundance (δ) in parts per mil (‰) compared to the industry standards.

2.5 | Data Analysis and Sediment Source Apportionment

The means and standard deviations of the tracers in the samples were calculated for the two size fractions (<63 and <32 µm). The C:N ratios were calculated based on the total C:N values for the same samples. This relationship was not explored as a tracer variable.

The first stage of the sediment source fingerprinting involved an exploratory analysis using box plots to evaluate the conservativeness of the isotopes. Subsequently, the Kruskal–Wallis *H*-test ($p < 0.05$) and stepwise discriminant function analysis ($p < 0.05$) were applied to assess the discriminatory power for the sediment sources.

The concentration-dependent MixSIAR (Stock and Semmens 2016) model was applied to estimate the contributions of the sediment sources, using the "extreme" execution parameter of the Markov Chain Monte Carlo. Results are considered acceptable when the variables have Gelman–Rubin values less than 1.01. We used virtual mixtures to evaluate the modeled source apportionment. The virtual sample mixtures were generated from known relative proportions of the potential sources. Twenty-eight sets of virtual mixtures were defined for each tracer group to represent the full range of possible contributions from the three sampled sources. The modeled source contributions were then evaluated against the known inputs using Nash–Sutcliffe efficiency index (NSE), coefficient of determination (R^2), root mean square error (RMSE) and mean absolute error (MAE) as performance metrics of the models. R^2 and NSE range from 0 to 1, with values closer to 1 indicating better model performance and stronger agreement between simulated and observed data. All modeling procedures were conducted using R software.

3 | Results

3.1 | Distribution of Carbon and Nitrogen and Their Respective Isotopic Ratios

The TC content in the <63 µm fraction of the source samples exhibited the following decreasing order: soils under SC (1.6% ± 0.4), CB (1.3% ± 0.4), and UR (0.7% ± 0.3) (Table 1). However, in the <32 µm fraction, TC followed this sequence: CB (2.5% ± 0.5) > SC (2.1% ± 0.4) > UR (1.0% ± 0.4). The same patterns were observed for TN in both fractions. In the <63 µm fraction, CB exhibited 0.18% (±0.05) TN, higher than soils under SC and UR, which had 0.15% (±0.04) and 0.08% (±0.03) TN, respectively. In the <32 µm fraction, CB, soils under SC, and UR had 0.24%, 0.18%, and 0.10% TN, respectively. The average C:N ratio in the sources for the <32 µm fraction decreased in the following order: soils under SC (12.1 ± 1.6), CB (10.6 ± 1.2), and UR (10.1 ± 1.1). However, this order differed in the <63 µm fraction: soils under SC (11 ± 1.9), UR (8.5 ± 2), and CB (7.4 ± 0.9).

The isotopic compositions of C and N associated with the two absolute particle size fractions of the source soil and suspended sediment samples varied considerably (Table 1). The mean values of $\delta^{13}C$ were higher in soils under SC (–18.80‰ ± 1.5 in the <32 µm fraction and –18.04‰ ± 1.4 in the <63 µm fraction) for both fractions, followed, respectively, by UR (–21.96‰ ± 2.0 in the <32 µm fraction and –21.42‰ ± 1.4 in the <63 µm fraction) and CB (–22.70‰ ± 1.7 in the <32 µm fraction and –22.83‰ ± 1.9 in the <63 µm fraction). CB exhibited 7.76‰ ± 1.5 of $\delta^{15}N$ in the <63 µm fraction, which was higher than in soils under SC and UR, which had 6.27‰ ± 1.5 and 5.32‰ ± 1.7, respectively. In the <32 µm fraction, CB showed the highest mean values of $\delta^{15}N$ (7.95‰ ± 1.2), followed by UR (6.08‰ ± 2.0) and SC (6.07‰ ± 1.4), respectively.

All the average TC and TN values in the source and target sediment samples were higher in the <32 µm fraction compared to the <63 µm fraction. For TC, the enrichment ratios in the fractions (<32 µm fraction/<63 µm fraction) followed the following order: CB (1.87) > BS (1.69) > UR (1.45) > SC (1.33) > SS (1.14). A similar pattern was identified for TN, although with slightly lower enrichment magnitudes. CB (1.33) also showed the highest TN enrichment, followed by UR and BS (both with 1.25). SC (1.20) and SS (1.05) exhibited the lowest TN enrichment values among the fractions. This pattern was maintained for $\delta^{15}N$, except for the average values in soils under SC. However, it was not evident for $\delta^{13}C$, which showed higher values in the <63 µm fraction. Although statistical differences were not tested, these contrasts between the size fractions were considered consistent with enrichment patterns, based on the known behavior of the individual tracers.

The mean TC content in the <32 µm fraction of BS was 2.81%, higher than the corresponding average for target SS, which was 2.38% (Table 1). The TN in SS and BS for the <32 µm fraction were similar; i.e., 0.25% and 0.23%, respectively. The mean contents of TC and TN in the <63 µm fraction were slightly higher in SS, presenting as 2.09% and 0.22%, respectively, compared to

TABLE 1 | Means and standard deviations (SD) of total carbon (TC) and total nitrogen (TN) contents, and $\delta^{13}C$ and $\delta^{15}N$ values in soils under sugarcane cultivation (SC), unpaved roads (UR), and channel banks (CB), as well as in target sediment samples (suspended sediments [SS] and bed sediments [BS]). Twenty-six from SC, 13 from UR, and 12 from eroding CB.

Tracers		Sugarcane cultivation ($n=26$)	Unpaved roads ($n=13$)	Channel banks ($n=12$)	Suspended sediment ($n=5$)	Bed sediment ($n=9$)
$<63\,\mu m$ fraction						
TC (%)	Mean	1.61	0.69	1.34	2.09	1.66
	SD	0.36	0.33	0.38	0.66	0.79
TN (%)	Mean	0.15	0.08	0.18	0.22	0.2
	SD	0.04	0.03	0.05	0.06	0.1
$\delta^{13}C$ (‰)	Mean	−18.04	−21.42	−22.83	−21.92	−24.22
	SD	1.4	1.38	1.87	2.41	1.36
$\delta^{15}N$ (‰)	Mean	6.27	5.32	7.76	7.14	7.88
	SD	1.48	1.73	1.46	0.4	1.93
$<32\,\mu m$ fraction						
TC (%)	Mean	2.14	1	2.5	2.38	2.81
	SD	0.44	0.41	0.5	0.81	0.91
TN (%)	Mean	0.18	0.1	0.24	0.23	0.25
	SD	0.04	0.03	0.06	0.06	0.08
$\delta^{13}C$ (‰)	Mean	−18.8	−21.96	−22.7	−21.94	−23.55
	SD	1.52	2	1.68	2.43	1.5
$\delta^{15}N$ (‰)	Mean	6.07	6.08	7.95	7.19	8.17
	SD	1.44	1.98	1.19	0.31	1.15

BS, which had 1.66% and 0.20%, respectively. The average C:N ratio of SS (10.2 and 9.5 in the <63 and $<32\,\mu m$ fractions, respectively) and BS (11.1 and 8.2 in the <63 and $<32\,\mu m$ fractions, respectively) was similar, with a decrease in this ratio in the $<63\,\mu m$ fraction. The mean values of $\delta^{13}C$ in SS (−21.94‰ and −21.92‰ in the <32 and $<63\,\mu m$ fractions, respectively) were higher than those in BS (−23.55‰ and −24.22‰ in the <32 and $<63\,\mu m$ fractions, respectively). However, the $\delta^{15}N$ in SS (7.19‰ and 7.14‰ in the <32 and $<63\,\mu m$ fractions, respectively) and BS (8.17‰ and 7.88‰ in the <32 and $<63\,\mu m$ fractions, respectively) were similar.

3.2 | Tracer Conservation Tests

$\delta^{13}C$ and $\delta^{15}N$ isotopes showed an acceptable pattern of conservativeness, as shown by the boxplots in Figure 3, wherein the values in the target sediment samples, except the outliers, ranged within the limits of the source samples.

3.3 | Composite Fingerprint Selection

$\delta^{13}C$ and $\delta^{15}N$ isotopes demonstrated the potential for source discrimination, as indicated by the Kruskal–Wallis H-test ($p<0.05$) (Table S1). The optimal tracer compositions selected by the LDA were capable of discriminating the sediment sources using both absolute particle size fractions (Table 2). The Wilks' lambda values and cumulative error of the discriminant analysis were more significant in the $<63\,\mu m$ fraction (Table 2). The results illustrated in Figure S1 showed that the dispersion of samples near the centroid was lower, and the distance from the centroid between sources was greater for the $<63\,\mu m$ fraction.

3.4 | Evaluating the Accuracy of the Source Apportionment Models

The results of the virtual mixtures showed that estimates of sediment source contributions were more reliable for the $<63\,\mu m$ fraction, as evidenced by significantly lower RMSE and MAE values and higher NSE values compared to the $<32\,\mu m$ fraction. On average, the NSE, RMSE, and MAE values for the <63 and $<32\,\mu m$ fractions were 0.82, 8.80 and 7.76, and 0.60, 12.49 and 11.12, respectively. The mean NSE value for the $<32\,\mu m$ fraction indicated potential uncertainties in the estimates for this fraction. These results also revealed greater reliability in the contributions of CB in both fractions and poor performance in the estimation of SC and UR in the $<32\,\mu m$ fraction (Table S2). The r^2 results were similar for both fractions.

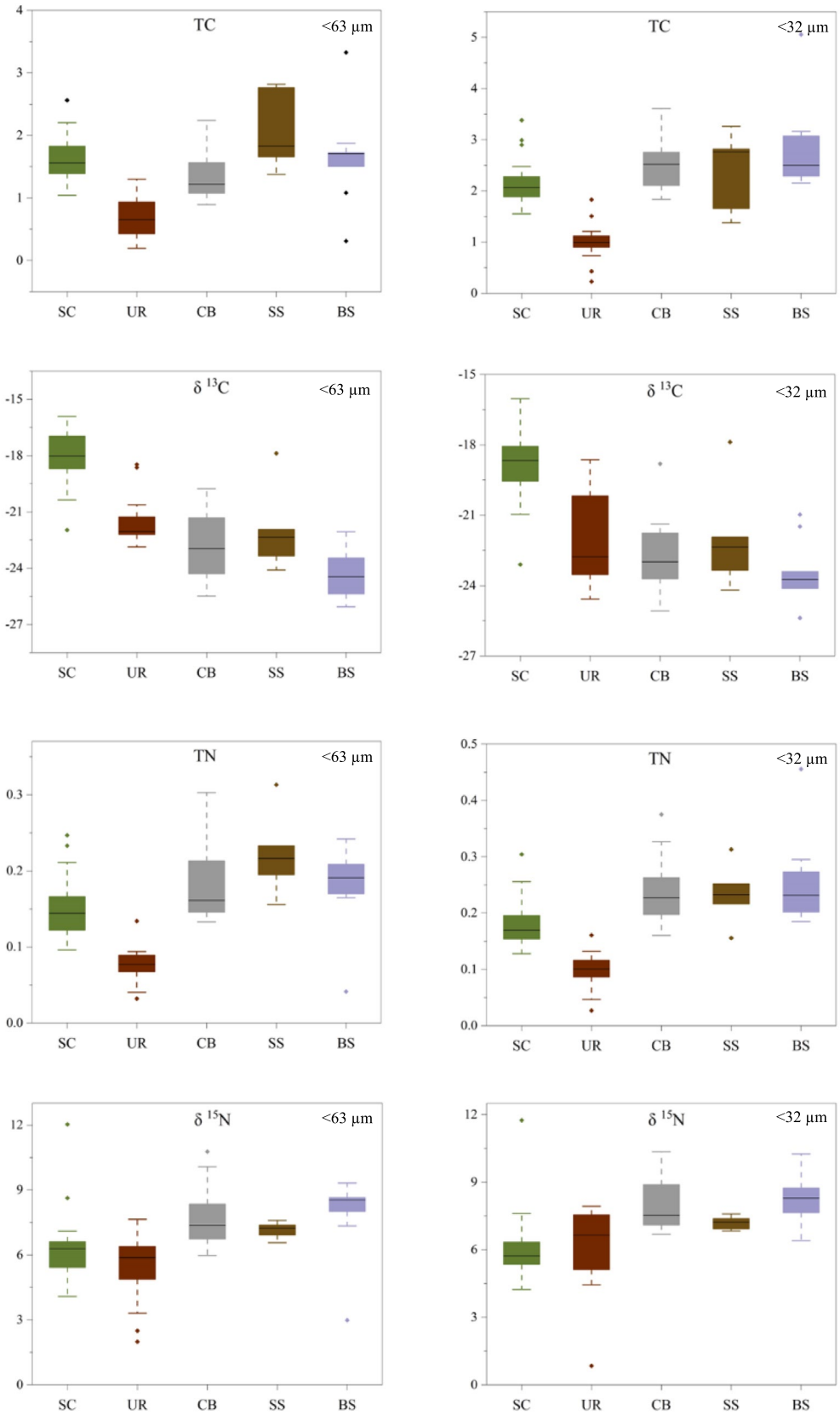

FIGURE 3 | Boxplot of total carbon (TC) (%), total nitrogen (TN) (%), $\delta^{13}C$ (‰), and $\delta^{15}N$ (‰) in sources and target sediment samples for the < 63 and < 32 µm fractions. BS, bed sediments; CB, channel banks; SC, sugarcane cultivation, SS, suspended sediments (SS); UR, unpaved roads. [Colour figure can be viewed at wileyonlinelibrary.com]

TABLE 2 | Results of linear discriminant analysis for the source < 63 and < 32 μm fractions.

Properties	Wilks' lambda	*F*	*p*	Error rates (%)
< 63 μm				
$\delta^{13}C$	0.33	48.28	0	19.61
$\delta^{15}N$	0.25	23.47	0.002	15.68
< 32 μm				
$\delta^{13}C$	0.45	28.3	0	35.29
$\delta^{15}N$	0.35	15.94	0	25.49

3.5 | Sediment Source Ascription

The results showed that CB is the most important source for the sampled sediments for both particle size fractions (Figure 4). In general, CB contributed 72% (±14) of the < 63 μm and 71% (±14) of the < 32 μm fraction of BS compared with 62% (±19) of the < 63 μm and 60% (±18) of the < 32 μm fraction of SS. The UR source was the second most important source of sampled sediments in the study basin, contributing 21% (±15) of the < 63 μm and 19% (±14) of the < 32 μm fractions of BS, and 26% (±18) of the < 63 μm and 23% (±17) of the < 32 μm fraction in the sampled SS.

CB was the primary source in most of the target sediment samples across the basin, especially in the bed sediment (BS), regardless of the soil context (Figure 5). In the < 63 μm fraction, only two bed sediment samples—one from the lower course and one from the upper course of the river—did not have the channel bank contributing more than 50% of the sampled sediment. The < 32 μm fraction exhibited similar variability in source contributions; CB was the main source in all sediment samples, and only two of them had a CB contribution below 50%—one in the middle course and one in the lower course of the main river.

4 | Discussion

Several studies have used combinations of TC, TN, $\delta^{13}C$, and $\delta^{15}N$ for sediment source apportionment (Mahoney et al. 2019; Riddle et al. 2025). Fox and Papanicolaou (2007) used for the first time $\delta^{13}C$, $\delta^{15}N$, and the TC to TN atomic ratio (C:N) as natural tracers for investigating the temporal and spatial variability of erosion processes, allowing for the distinction between agricultural hillslopes and floodplain sediment contributions. Fox (2009) analyzed TC, TN, $\delta^{13}C$, and $\delta^{15}N$ for their ability to elucidate the impact of surface coal mining on sediment transportation, reporting satisfactory results for $\delta^{13}C$ and $\delta^{15}N$ in differentiating erosion of channel banks and surface soils.

However, the sediment source discrimination power of such tracers may vary among different environmental settings and source classifications. In their research of sediment source apportionment, Stewart et al. (2015) applied $\delta^{13}C$ and $\delta^{15}N$ isotopes along with elemental profiles for the discrimination of channel banks, forests, roads, and croplands. In their study area, the sources exhibited similarity in their isotopic signatures, pointing to the inclusion of $\delta^{13}C$ and $\delta^{15}N$ isotopes slightly increasing the uncertainty in source discrimination and apportionment. Here, it is a well-known fact that tracers must differ significantly between sources for robust source apportionment. In the case of our study herein, the sources have clearly presented similar distribution patterns for TN, $\delta^{13}C$, and $\delta^{15}N$ in both the < 32 and < 63 μm fractions (Table 1).

Issues of nonstationarity and conservation of isotopic composition in sediments are commonly reported in this type of study (Fox and Martin 2015). The accumulation of algae in sediments during river transport is one of the main factors contributing

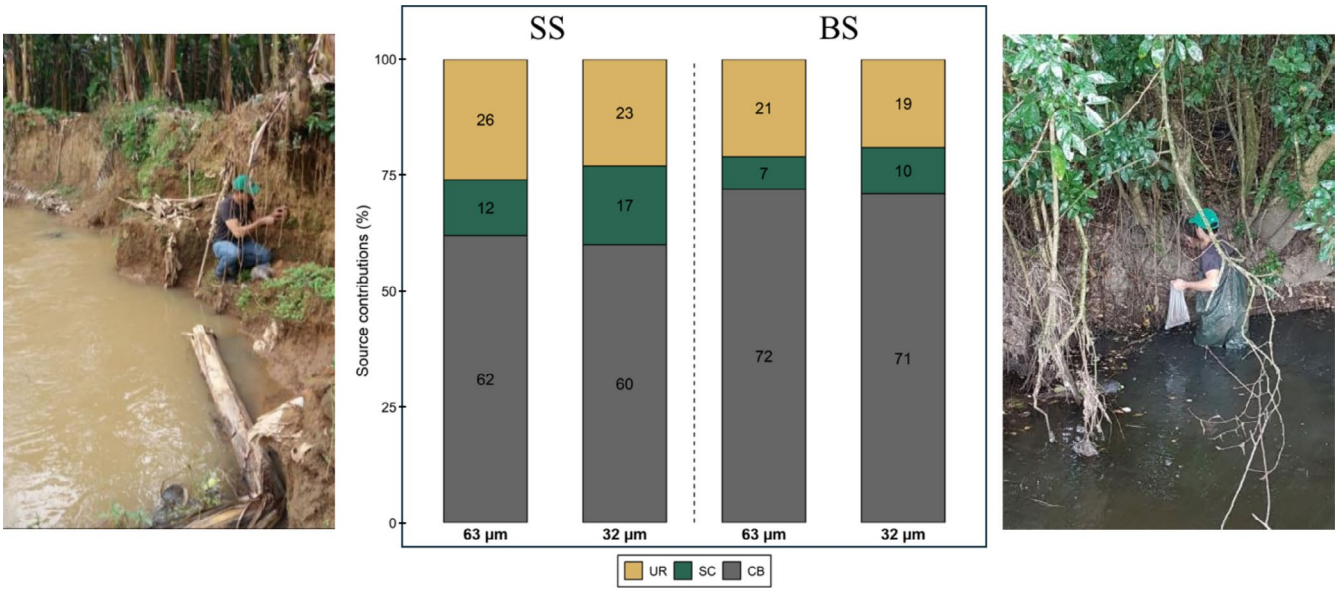

FIGURE 4 | Overall mean results of source contributions to sampled suspended sediment (SS) and bed sediment (BS). Sampled sediment sources: sugarcane cultivation (SC), unpaved roads (UR), and channel banks (CB). [Colour figure can be viewed at wileyonlinelibrary.com]

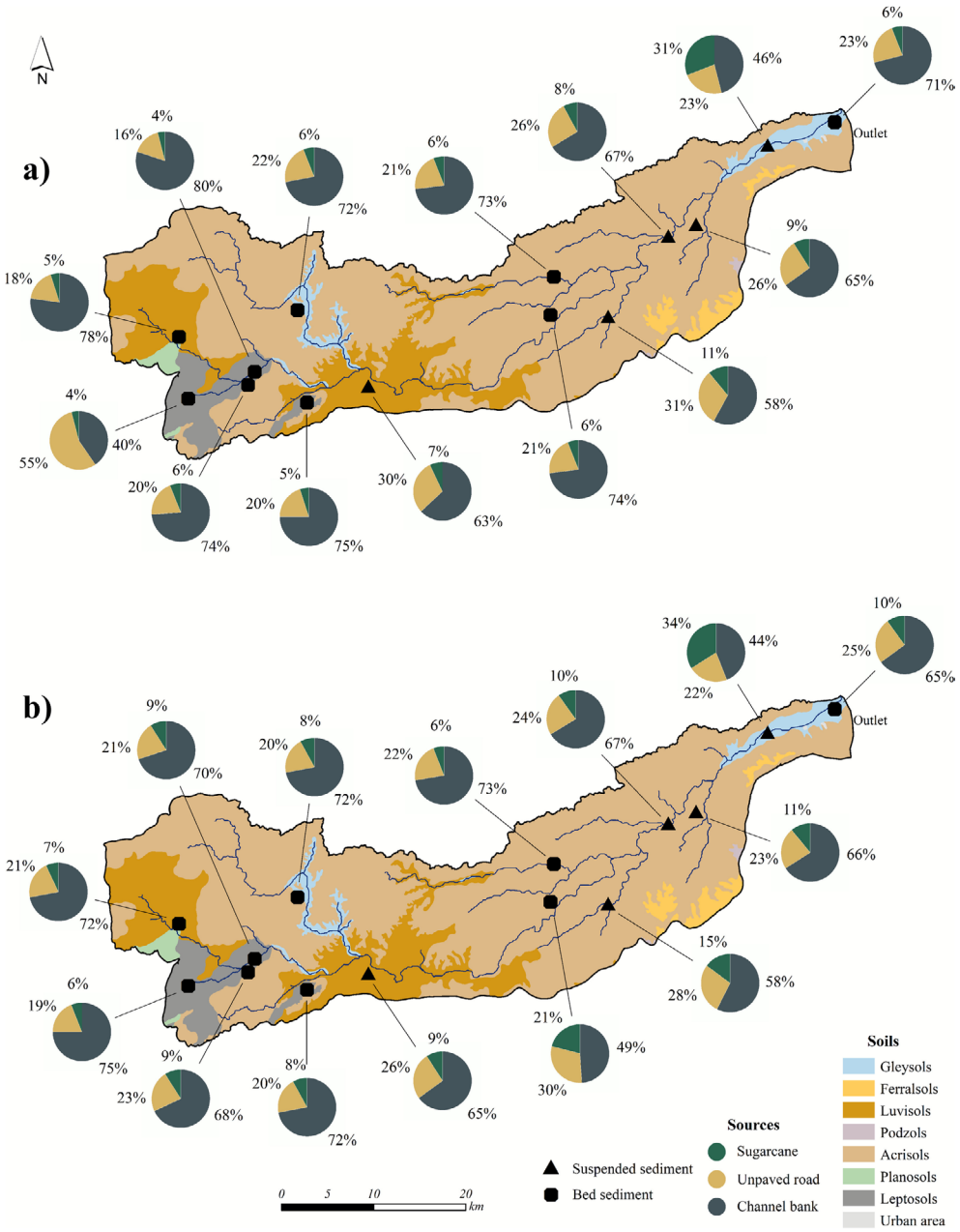

FIGURE 5 | Source contributions to the $<63\,\mu m$ (a) and $<32\,\mu m$ (b) fractions of suspended and bed sediments, imposed on a map showing soil distribution within the study basin. [Colour figure can be viewed at wileyonlinelibrary.com]

to the low conservation of $\delta^{13}C$ and $\delta^{15}N$. Algae, due to their composition, can lower the isotopic ratios of $\delta^{13}C$ and $\delta^{15}N$ in sediments, given that these species exhibit ratios in the range of −38‰ (Riddle et al. 2022). In the case of the study reported herein, the average C:N ratio, an indicator of algae accumulation, in both target sediment size fractions was generally less than 10, suggesting widespread stabilization of unicellular algae (Baird and Middleton 2004).

Our study area is located in a region in which the agricultural activities are mainly focused on sugarcane production. This is a historically established monoculture. The first records of sugarcane cultivation in the Zona da Mata region of Pernambuco, where the basin is located, date back to the late 16th century and persist to the present day (Morais 2022). Monoculture remains a defining feature of this region, with no significant evidence of crop rotation practices. Consequently, sugarcane cultivation represents the dominant isotopic signature in the agricultural soils of the study catchment.

The isotopic signatures of $\delta^{13}C$ and $\delta^{15}N$ are connected to specific sugarcane features, which is a C_4-type plant involved in symbiosis with N_2-fixing bacteria (Biggs et al. 2002). The usage of $\delta^{15}N$ in research as a feature related to sugarcane cultivations is a common approach. It has, for instance, been used to measure N pollution from fertilized sugarcane in wetlands (Lindau et al. 1997), to identify the sources of nitrate at watershed scale (Jin et al. 2020), and to investigate N_2-fixation associated with sugarcane plants (Monteiro et al. 2021; Boddey et al. 2001). Research approaches using $\delta^{13}C$ are also common in the context

of sugarcane cultivations. It has been used as a discriminator to evaluate the response of sugarcane to N-fertilization (Kölln et al. 2016) and to assess the impact of management and harvesting methods on soil organic C stocks (Brandani et al. 2014). The use of $\delta^{13}C$ has also been reported for discriminating the contribution of particulate organic C to water between sugarcane cultivations and riparian vegetation areas (Gomes et al. 2019). It is important to note that the land use change from native vegetation to sugarcane cultivations has the potential to change the $\delta^{13}C$ and $\delta^{15}N$ soil profiles (Rossi et al. 2013), raising the importance of such tracers for discriminating sugarcane cultivations as distinctive sediment sources.

The enrichment of $\delta^{13}C$ in surface soils under SC, compared to other sources, was expected since the organic matter in these soils mainly originates from C_4-type plants (Campbell et al. 2009). This pattern was even more evident for particles $<63\,\mu m$, given that the variation in the ^{13}C ratio between the UR and CB sources was lower in the $<32\,\mu m$ fraction. During the transformations of soil carbon, there is an isotopic enrichment of ^{13}C for the more recalcitrant organic matter products. UR and CB samples showed significantly lower $\delta^{13}C$ values compared to SC, which was typically above −20‰. In our study catchment, these two former sources were mostly characterized using subsurface layers, whereas the SC samples comprised topsoil.

It is important to acknowledge that, even though our results demonstrated that the tracers effectively discriminate between the sampled sources, the Kruskal–Wallis *H*-test (Table S1) revealed interesting patterns regarding the discriminative ability of each individual tracer between different source pairs. For both absolute particle size fractions, $\delta^{13}C$ did not effectively discriminate between CB and UR, indicating a similar $\delta^{13}C$ signature for this specific pair of sources. This similarity is likely related to the comparable nature of CB and UR, as both represent subsurface soil layers. In contrast, the SC samples correspond to the surface layer influenced by C_4-type vegetation, which, as previously noted, enriches soil organic matter and thereby modulates the $\delta^{13}C$ composition. $\delta^{15}N$ did not significantly discriminate between SC and UR. In contrast, for the CB and SC pairing, and across both particle size fractions, the $\delta^{13}C$ and $\delta^{15}N$ tracers showed clear discriminatory power ($p < 0.01$).

Laceby et al. (2014) successfully combined geochemical composition, $\delta^{13}C$, and $\delta^{15}N$ as tracers to differentiate CB erosion from gully erosion. Their specific work noted that sediment properties related to N showed considerable enrichment in particle size fractions and substantial temporal variation, suggesting nonconservative behavior. On the other hand, stable C isotopes exhibited minimal variation with respect to both particle size and time, underscoring their effectiveness for sediment source tracing purposes. The same authors pointed out the limitations of using $\delta^{13}C$ and $\delta^{15}N$ without the addition of TN and TC contents. In contrast, McCarney-Castle et al. (2017) used $\delta^{13}C$ and $\delta^{15}N$ alone as tracers for discriminating urban areas, forested areas, and channel banks as sediment sources, reporting reliable results. However, such success could be related to a specific environmental setting that favors the potential of $\delta^{13}C$ and $\delta^{15}N$ as tracers. Overall, our results further underscore the potential of combining $\delta^{13}C$ and $\delta^{15}N$ with TC and TN as robust composite fingerprints for delivering reliable outcomes from sediment source modeling.

The two particle fractions showed no significant differences during the modeling in terms of tracer conservativeness and estimates of relative contributions. The $<63\,\mu m$ fraction showed better discrimination potential, with lower Wilks' lambda and cumulative error values in the discriminant analysis. This fraction also produced more reliable estimates, indicated by higher r^2 and NSE values and lower RMSE and MAE values (Table 3). Future studies and monitoring of sediment transport processes could focus on a single target sediment size fraction. The $<63\,\mu m$ fraction generally represents a larger volume of transported particles, while the $<32\,\mu m$ fraction may present a higher risk for poor source discrimination, particularly between CB and UR.

4.1 | Sediment Delivery Patterns

CB were identified as the predominant sources of SS and BS, contributing between 60% and 72% of the total sediment load, followed by SC and UR. Our results align with patterns found in other river catchments within the same tropical region (Amorim et al. 2021; Nascimento et al. 2024). The high contribution of CB can largely be attributed to the absence and type of vegetation cover, an essential factor for stabilizing riverbanks (Henriques et al. 2022). At many CB sampling points, either sparse ground cover, complete bank face exposure, or a lack of vegetation in the riparian zone was observed, despite Brazilian environmental legislation recommending the preservation of native Atlantic Forest vegetation in these areas of river catchments (Guidotti et al. 2020).

An indirect factor that can influence the contribution of CB is the lower slope of the land in areas cultivated with SC. The downstream portion of the catchment is part of the coastal plain, characterized by slopes of 0%–3%. In the upstream portion, altitudes reach 700 m, with steeper slopes reflecting the geomorphological complexity of the area under study herein. This pattern contrasts with the SC areas in the Ipojuca River

TABLE 3 | Results of virtual mixture tests using the Nash–Sutcliffe efficiency index (NSE), coefficient of determination (r^2), root mean square error (RMSE), and mean absolute error (MAE).

Selected tracers	Sources	NSE	R^2	RMSE	MAE
$<63\,\mu m$ fraction	SC	0.88	0.97	7.31	6.04
	UR	0.67	0.95	12.27	11.39
	CB	0.90	0.96	6.81	5.85
	Global	0.82	0.82	8.80	7.76
$<32\,\mu m$ fraction	SC	0.40	0.95	16.49	14.45
	UR	0.43	0.89	16.14	14.88
	CB	0.95	0.95	4.84	4.04
	Global	0.60	0.64	12.49	11.12

Abbreviations: CB, channel banks; SC, sugarcane cultivation; UR, unpaved roads.

catchment, where the more steeply sloping terrain favors a higher contribution from this crop (Nascimento et al. 2023). The geomorphological difference between these regions may explain the lower rate of surface soil erosion in areas with gentle slopes, which increases the relative contribution of CB (Nascimento et al. 2023).

The highest CB contributions were observed in samples from the upper reaches of the basin (6 BS and 1 SS), ranging from 40% to 80% for the $<63\,\mu m$ fraction (Figure 5A) and from 65% to 75% for the $<32\,\mu m$ fraction (Figure 5B). In this context, targeted management measures can be implemented along the banks to reduce sediment input. Structural engineering solutions, which are often costly, have been increasingly replaced by more sustainable approaches to address riverbank erosion and instability (Mondal and Patel 2020). Restoring riparian vegetation promotes greater ecological integration with minimal environmental impact and may be the most effective medium- to long-term strategy for all river courses in the basin, particularly in the upstream stretches (Cole et al. 2020; Del Tánago et al. 2021). This practice enhances bank stability through a root structure that increases surface roughness and resistance to particle transport, thereby reducing erosion in adjacent areas (Julian and Torres 2006). The Atlantic Forest vegetation, a biome native to the region, is characterized by large trees, dense canopy cover, and deep root systems.

Several countries have adopted specific policies to protect riverbanks as a crucial measure to tackle river erosion and reduce sediment transport. While their approaches vary, these policies commonly recognize riparian zones as essential ecological infrastructures for controlling soil loss and supporting other ecological functions. In the European Union, the Water Framework Directive (2000/60/EC) mandates the preservation or restoration of riparian zones, particularly in basins with intensive land use. However, each member state typically develops its own guidelines tailored to its unique environmental, climatic, and socioeconomic conditions. In the United States, regulation occurs at multiple levels of government—federal, state, and local. At the federal level, the Conservation Reserve Program (CRP), managed by the Department of Agriculture (USDA), provides financial incentives for landowners to maintain riparian vegetation strips for periods of 10–15 years. In areas with intensive agriculture, buffer strips ranging from 10 to 100 m are particularly important.

In Brazil, the Forest Code (Law 12.651/2012) mandates the obligatory preservation of Permanent Preservation Areas (PPAs) along surface waters, with minimum widths varying according to the size of the water body. In this catchment where the main river width ranges between 10 and 20 m, a minimum strip of 50 m of native vegetation must be maintained on each bank. Illegal deforestation of riparian zones in Brazil is subject to enforcement by environmental agencies and may result in fines, activity embargoes, or mandatory environmental restoration.

5 | Conclusion

Our results showed that $\delta^{13}C$ and $\delta^{15}N$ met the criteria for effective modeling of sediment source contributions, providing a high level of detail on sediment delivery patterns in a tropical catchment under intensive land use. The analyses carried out on two absolute particle size fractions showed specific patterns of tracer enrichment and conservation, while also effectively discriminating the individual sediment sources, mainly in the fraction $<63\,\mu m$. The results highlighted the dominance of CB as the main sediment source in both absolute particle size fractions. The substantial contribution of this source underscores that agricultural expansion into fragile riparian zones has accelerated soil loss—particularly in areas with inadequate bank management and insufficient protective vegetation—thereby threatening land productivity and water quality. Therefore, we underscore the need for more detailed studies on the effectiveness of bank reforestation in tandem with current Brazilian legislation for designing land-degradation mitigation strategies. Our study herein also highlights the importance of developing innovative, interdisciplinary approaches to effectively manage and integrate riparian vegetation into landscape planning and water resource strategies.

Acknowledgments

The first author was supported (Fellowship and PDSE-20187604752) by the Coordination for the Improvement of Higher Education Personnel (CAPES). Y.J.A.B. da Silva is grateful to the National Council for Scientific and Technological Development – CNPq for research productivity scholarship (Process Number: 303323/2022-1). Rothamsted Research receives strategic funding from the UKRI-BBSRC (UK Research and Innovation-Biotechnology and Biological Sciences Research Council) and the contribution of Y.Z., S.P., H.R.U., and A.L.C. to this paper was specifically funded by grant award BB/X010961/1—specifically work package 2—BBS/E/RH/230004B; Detecting agroecosystem "resilience" using novel data science methods. The analyses reported in this paper were undertaken at Rothamsted Research while FA was being co-supervised as a doctoral student by A.L.C. The Article Processing Charge for the publication of this research was funded by the Coordenação de Aperfeiçoamento de Pessoal de Nível Superior - Brasil (CAPES) (ROR identifier: 00x0ma614).

Funding

The first author was supported (Fellowship and PDSE-20187604752) by the Coordination for the Improvement of Higher Education Personnel (CAPES). The corresponding author was supported by the National Council for Scientific and Technological Development (CNPq - Process Number 303323/2022-1). Rothamsted Research receives strategic funding from the UKRI-BBSRC (UK Research and Innovation-Biotechnology and Biological Sciences Research Council) and the contribution of Y.Z., S.P., H.R.U., and A.L.C. to this paper was specifically funded by grant award BB/X010961/1—specifically work package 2—BBS/E/RH/230004B; Detecting agroecosystem "resilience" using novel data science methods. The analyses reported in this paper were undertaken at Rothamsted Research while FA was being co-supervised as a doctoral student by A.L.C.

Data Availability Statement

The data that support the findings of this study are available on request from the corresponding author. The data are not publicly available due to privacy or ethical restrictions.

References

Abbas, G., S. Jomaa, P. Fink, et al. 2024. "Investigating Sediment Sources Using Compound-Specific Stable Isotopes and Conventional

Fingerprinting Methods in an Agricultural Loess Catchment." *Catena* 246: 108336. https://doi.org/10.1016/j.catena.2024.108336.

Amorim, F. F., Y. J. A. B. da Silva, R. C. Nascimento, et al. 2021. "Sediment Source Apportionment Using Optical Property Composite Signatures in a Rural Catchment, Brazil." *Catena* 202: 105208. https://doi.org/10.1016/j.catena.2021.105208.

Bahadori, M., C. Chen, S. Lewis, et al. 2019. "A Novel Approach of Combining Isotopic and Geochemical Signatures to Differentiate the Sources of Sediments and Particulate Nutrients From Different Land Uses." *Science of the Total Environment* 655: 129–140. https://doi.org/10.1016/j.scitotenv.2018.11.084.

Baird, M. E., and J. H. Middleton. 2004. "On Relating Physical Limits to the Carbon: Nitrogen Ratio of Unicellular Algae and Benthic Plants." *Journal of Marine Systems* 49, no. 1–4: 169–175. https://doi.org/10.1016/j.jmarsys.2003.10.007.

Batista, P. V., J. P. Laceby, and O. Evrard. 2022. "How to Evaluate Sediment Fingerprinting Source Apportionments." *Journal of Soils and Sediments* 22, no. 4: 1315–1328. https://doi.org/10.1007/s11368-022-03157-4.

Bender, M. M. 1971. "Variations in the $^{13}C/^{12}C$ Ratios of Plants in Relation to the Pathway of Photosynthetic Carbon Dioxide Fixation." *Phytochemistry* 10: 1239–1244.

Biggs, I. M., G. R. Stewart, J. R. Wilson, and C. Critchley. 2002. "^{15}N Natural Abundance Studies in Australian Commercial Sugarcane." *Plant and Soil* 238: 21–30. https://doi.org/10.1023/A:1014280420779.

Boddey, R. M., J. C. Polidoro, A. S. Resende, B. J. Alves, and S. Urquiaga. 2001. "Use of the ^{15}N Natural Abundance Technique for the Quantification of the Contribution of N_2 Fixation to Sugar Cane and Other Grasses." *Australian Journal of Plant Physiology* 28, no. 9: 889–895. https://doi.org/10.1071/PP01058.

Brandani, C. B., T. F. Abbruzzini, S. Williams, M. Easter, C. E. Pellegrino Cerri, and K. Paustian. 2014. "Simulation of Management and Soil Interactions Impacting SOC Dynamics in Sugarcane Using the CENTURY Model." *GCB Bioenergy* 7, no. 4: 646–657. https://doi.org/10.1111/gcbb.12175.

Campbell, J. E., J. F. Fox, C. M. Davis, H. D. Rowe, and N. Thompson. 2009. "Carbon and Nitrogen Isotopic Measurements From Southern Appalachian Soils: Assessing Soil Carbon Sequestration Under Climate and Land-Use Variation." *Journal of Environmental Engineering* 135, no. 6: 439–448. https://doi.org/10.1061/(ASCE)EE.1943-7870.0000008.

Cole, L. J., J. Stockan, and R. Helliwell. 2020. "Managing Riparian Buffer Strips to Optimise Ecosystem Services: A Review." *Agriculture, Ecosystems & Environment* 296: 106891. https://doi.org/10.1016/j.agee.2020.106891.

Collins, A. L., M. Blackwell, P. Boeckx, et al. 2020. "Sediment Source Fingerprinting: Benchmarking Recent Outputs, Remaining Challenges and Emerging Themes." *Journal of Soils and Sediments* 20: 4160–4193. https://doi.org/10.1007/s11368-020-02755-4.

Collins, A. L., E. Burak, P. Harris, S. Pulley, L. Cardenas, and Q. Tang. 2019. "Field Scale Temporal and Spatial Variability of $\delta^{13}C$, $\delta^{15}N$, TC and TN Soil Properties: Implications for Sediment Source Tracing." *Geoderma* 333: 108–122. https://doi.org/10.1016/j.geoderma.2018.07.019.

Collins, A. L., S. Pulley, I. D. Foster, A. Gellis, P. Porto, and A. J. Horowitz. 2017. "Sediment Source Fingerprinting as an Aid to Catchment Management: A Review of the Current State of Knowledge and a Methodological Decision-Tree for End-Users." *Journal of Environmental Management* 194: 86–108. https://doi.org/10.1016/j.jenvman.2016.09.075.

Collins, A. L., and D. E. Walling. 2004. "Documenting Catchment Suspended Sediment Sources: Problems, Approaches and Prospects." *Progress in Physical Geography* 28, no. 2: 159–196. https://doi.org/10.1191/0309133304pp409ra.

Dąbrowska, J., P. B. Dąbek, and I. Lejcuś. 2018. "Identifying Surface Runoff Pathways for Cost-Effective Mitigation of Pollutant Inputs to Drinking Water Reservoir." *Water* 10, no. 10: 1300. https://doi.org/10.3390/w10101300.

Dalzell, B. J., T. R. Filley, and J. M. Harbor. 2007. "The Role of Hydrology in Annual Organic Carbon Loads and Terrestrial Organic Matter Export From a Midwestern Agricultural Watershed." *Geochimica et Cosmochimica Acta* 71, no. 6: 1448–1462. https://doi.org/10.1016/j.gca.2006.12.009.

Davis, C. M., and J. F. Fox. 2009. "Sediment Fingerprinting: Review of the Method and Future Improvements for Allocating Nonpoint Source Pollution." *Journal of Environmental Engineering* 135, no. 7: 490–504. https://doi.org/10.1061/(ASCE)0733-9372(2009)135:7(490).

Deasy, C., R. E. Brazier, A. L. Heathwaite, and R. Hodgkinson. 2009. "Pathways of Runoff and Sediment Transfer in Small Agricultural Catchments." *Hydrological Processes* 23, no. 9: 1349–1358. https://doi.org/10.1002/hyp.7257.

Del Tánago, M. G., V. Martínez-Fernández, F. C. Aguiar, et al. 2021. "Improving River Hydromorphological Assessment Through Better Integration of Riparian Vegetation: Scientific Evidence and Guidelines." *Journal of Environmental Management* 292: 112730. https://doi.org/10.1016/j.jenvman.2021.112730.

Evrard, O., J. P. Laceby, G. F. Ficetola, et al. 2019. "Environmental DNA Provides Information on Sediment Sources: A Study in Catchments Affected by Fukushima Radioactive Fallout." *Science of the Total Environment* 665: 873–881. https://doi.org/10.1016/j.scitotenv.2019.02.191.

Fox, J. F. 2009. "Identification of Sediment Sources in Forested Watersheds With Surface Coal Mining Disturbance Using Carbon and Nitrogen Isotopes." *Journal of the American Water Resources Association* 45, no. 5: 1273–1289. https://doi.org/10.1111/j.1752-1688.2009.00365.x.

Fox, J. F., and D. K. Martin. 2015. "Sediment Fingerprinting for Calibrating a Soil Erosion and Sediment-Yield Model in Mixed Land-Use Watersheds." *Journal of Hydrologic Engineering* 20, no. 6: C4014002. https://doi.org/10.1061/(ASCE)HE.1943-5584.0001011.

Fox, J. F., and A. N. Papanicolaou. 2007. "The Use of Carbon and Nitrogen Isotopes to Study Watershed Erosion Processes." *Journal of the American Water Resources Association* 43, no. 4: 1047–1064. https://doi.org/10.1111/j.1752-1688.2007.00087.x.

Gaspar, L., W. H. Blake, I. Lizaga, B. Latorre, and A. Navas. 2022. "Particle Size Effect on Geochemical Composition of Experimental Soil Mixtures Relevant for Unmixing Modelling." *Geomorphology* 403: 108178. https://doi.org/10.1016/j.geomorph.2022.108178.

Gellis, A. C., W. W. Emmett, and L. B. Leopold. 2005. "Channel and Hillslope Processes Revisited in the Arroyo de Los Frijoles Watershed Near Santa Fe, New Mexico." *United States Geological Survey Professional Paper* 1704: 53.

Gellis, A. C., C. C. Fuller, P. Van Metre, et al. 2019. "Combining Sediment Fingerprinting With Age-Dating Sediment Using Fallout Radionuclides for an Agricultural Stream, Walnut Creek, Iowa, USA." *Journal of Soils and Sediments* 19: 3374–3396. https://doi.org/10.1007/s11368-018-2168-z.

Gomes, T. F., M. de Van Broek, G. Govers, et al. 2019. "Runoff, Soil Loss, and Sources of Particulate Organic Carbon Delivered to Streams by Sugarcane and Riparian Areas: An Isotopic Approach." *Catena* 181: 104083. https://doi.org/10.1016/j.catena.2019.104083.

Guidotti, V., S. F. Barros Ferraz, L. F. G. Pinto, et al. 2020. "Changes in Brazil's Forest Code Can Erode the Potential of Riparian Buffers to Supply Watershed Services." *Land Use Policy* 94: 104511. https://doi.org/10.1016/j.landusepol.2020.104511.

Guo, Y., C. Peng, Q. Zhu, et al. 2019. "Modelling the Impacts of Climate and Land Use Changes on Soil Water Erosion: Model Applications, Limitations and Future Challenges." *Journal of Environmental Management* 250: 109403. https://doi.org/10.1016/j.jenvman.2019.109403.

Haddadchi, A., D. S. Ryder, O. Evrard, and J. Olley. 2013. "Sediment Fingerprinting in Fluvial Systems: Review of Tracers, Sediment Sources and Mixing Models." *International Journal of Sediment Research* 28, no. 4: 560–578. https://doi.org/10.1016/S1001-6279(14)60013-5.

Henriques, M., T. R. McVicar, K. L. Holland, and E. Daly. 2022. "Riparian Vegetation and Geomorphological Interactions in Anabranching Rivers: A Global Review." *Ecohydrology* 15, no. 2: e2370. https://doi.org/10.1002/eco.2370.

Huang, C., Z. Zhou, M. Teng, C. Wu, and P. Wang. 2020. "Effects of Climate, Land Use and Land Cover Changes on Soil Loss in the Three Gorges Reservoir Area, China." *Geography and Sustainability* 1, no. 3: 200–208. https://doi.org/10.1016/j.geosus.2020.08.001.

IUSS Working Group WRB. 2006. *World Reference Base for Soil Resources 2006, World Soil*. FAO.

Jin, Z., J. Wang, J. Chen, et al. 2020. "Identifying the Sources of Nitrate in a Small Watershed Using δ15N-δ18O Isotopes of Nitrate in the Kelan Reservoir, Guangxi, China." *Agriculture, Ecosystems & Environment* 297: 106936. https://doi.org/10.1016/j.agee.2020.106936.

Julian, J. P., and R. Torres. 2006. "Hydraulic Erosion of Cohesive Riverbanks." *Geomorphology* 76, no. 1–2: 193–206.

Kölln, O. T., G. J. de Castro Gava, H. Cantarella, et al. 2016. "Fertigated Sugarcane Yield and Carbon Isotope Discrimination ($\Delta^{13}C$) Related to Nitrogen Nutrition." *Sugar Technology* 18: 391–400. https://doi.org/10.1007/s12355-015-0384-z.

Kopittke, P. M., N. W. Menzies, P. Wang, B. A. McKenna, and E. Lombi. 2019. "Soil and the Intensification of Agriculture for Global Food Security." *Environment International* 132: 105078. https://doi.org/10.1016/j.envint.2019.105078.

Laceby, J. P., J. Olley, T. J. Pietsch, F. Sheldon, and S. E. Bunn. 2014. "Identifying Subsoil Sediment Sources With Carbon and Nitrogen Stable Isotope Ratios." *Hydrological Processes* 29, no. 8: 1956–1971. https://doi.org/10.1002/hyp.10311.

Leite, F. F. G. D., A. Fontana, G. N. Nóbrega, et al. 2025. "Land Use Change Effect on Organic Matter Dynamics and Soil Carbon Sequestration in the Brazilian Cerrado: A Study Case in Mato Grosso Do Sul State (Midwest-Brazil)." *Catena* 249: 108670. https://doi.org/10.1016/j.catena.2024.108670.

Lindau, C. W., R. D. Delaune, and D. P. Alford. 1997. "Monitoring Nitrogen Pollution From Sugarcane Runoff Using ^{15}N Analysis." *Water, Air, and Soil Pollution* 98: 389–399. https://doi.org/10.1007/BF02047046.

Liu, K., D. A. Lobb, J. J. Miller, P. N. Owens, and M. E. Caron. 2017. "Determining Sources of Fine-Grained Sediment for a Reach of the Lower Little Bow River, Alberta, Using a Colour-Based Sediment Fingerprinting Approach." *Canadian Journal of Soil Science* 98, no. 1: 55–69. https://doi.org/10.1139/cjss-2016-0131.

Lizaga, I., B. Latorre, L. Gaspar, and A. Navas. 2022. "Combined Use of Geochemistry and Compound-Specific Stable Isotopes for Sediment Fingerprinting and Tracing." *Science of the Total Environment* 832: 154834.

Mahoney, D. T., N. Al Aamery, J. F. Fox, B. Riddle, W. Ford, and Y. T. Wang. 2019. "Equilibrium Sediment Exchange in the Earth's Critical Zone: Evidence From Sediment Fingerprinting With Stable Isotopes and Watershed Modeling." *Journal of Soils and Sediments* 19: 3332–3356. https://doi.org/10.1139/cjss-2016-0131.

Mariotti, A. 1983. "Atmospheric Nitrogen Is a Reliable Standard for Natural ^{15}N Abundance Measurements." *Nature* 303: 685–687. https://doi.org/10.1038/303685a0.

McCarney-Castle, K., T. M. Childress, and C. R. Heaton. 2017. "Sediment Source Identification and Load Prediction in a Mixed-Use Piedmont Watershed, South Carolina." *Journal of Environmental Management* 185: 60–69. https://doi.org/10.1016/j.jenvman.2016.10.036.

Mondal, S., and P. P. Patel. 2020. "Implementing Vetiver Grass-Based Riverbank Protection Programmes in Rural West Bengal, India." *Natural Hazards* 103, no. 1: 1051–1076. https://doi.org/10.1007/s11069-020-04025-5.

Montanarella, L., D. J. Pennock, N. McKenzie, et al. 2016. "World's Soils Are Under Threat." *Soil* 2, no. 1: 79–82. https://doi.org/10.5194/soil-2-79-2016.

Monteiro, E. D. C., C. G. N. Silva, M. dos reis Martins, et al. 2021. "Strategy for the Sampling of Sugarcane Plants for the Reliable Quantification of N_2 Fixation Using ^{15}N Natural Abundance." *Journal of Soil Science and Plant Nutrition* 21, no. 4: 2741–2752. https://doi.org/10.1007/s42729-021-00561-6.

Morais, A. L. D. S. 2022. "A Formação e Consolidação de um Grupo de Produtores de Açúcar da Nobreza da terra. Capitania de Pernambuco, Séculos XVI-XVIII." *Tempo* 28, no. 1: 178–197.

Muggler, C. C., T. Pape, and P. Buurman. 1997. "Laser Grain-Size Determination in Soil Genetic Studies 2. Clay Content, Clay Formation, and Aggregation in Some Brazilian Oxisols." *Soil Science* 162, no. 3: 219–228.

Mukundan, R., D. E. Walling, A. C. Gellis, M. C. Slattery, and D. E. Radcliffe. 2012. "Sediment Source Fingerprinting: Transforming From a Research Tool to a Management Tool 1." *Journal of the American Water Resources Association* 48, no. 6: 1241–1257. https://doi.org/10.1111/j.1752-1688.2012.00685.x.

Nascimento, R. C., A. J. Maia, P. H. S. D. Oliveira, et al. 2024. "Sugarcane Cultivation as a Major Surface Source of Sediment in Catchments From a Coastal Zone of Pernambuco, Brazil." *Revista Brasileira de Ciência do Solo* 48: e0230136. https://doi.org/10.36783/18069657rbcs20230136.

Nascimento, R. C., A. J. Maia, Y. J. A. B. Silva, et al. 2023. "Sediment Source Apportionment Using Geochemical Composite Signatures in a Large and Polluted River System With a Semiarid-Coastal Interface, Brazil." *Catena* 220: 106710. https://doi.org/10.1016/j.catena.2022.106710.

Nosrati, K., Z. Fathi, and A. L. Collins. 2019. "Fingerprinting Sub-Basin Spatial Suspended Sediment Sources by Combining Geochemical Tracers and Weathering Indices." *Environmental Science and Pollution Research* 26: 28401–28414. https://doi.org/10.1007/s11356-019-06024-x.

Papanicolaou, A. N., J. F. Fox, and J. Marshall. 2003. "Soil Fingerprinting in the Palouse Basin, USA, Using Stable Carbon and Nitrogen Isotopes." *International Journal of Sediment Research* 18, no. 2: 278–284.

Phillips, J. M., M. A. Russell, and D. E. Walling. 2000. "Time-Integrated Sampling of Fluvial Suspended Sediment: A Simple Methodology for Small Catchments." *Hydrological Processes* 14, no. 14: 2589–2602. https://doi.org/10.1002/1099-1085(20001015)14:14<2589.

Pulley, S., I. Foster, and A. L. Collins. 2017. "The Impact of Catchment Source Group Classification on the Accuracy of Sediment Fingerprinting Outputs." *Journal of Environmental Management* 194: 16–26. https://doi.org/10.1016/j.jenvman.2016.04.048.

Puntenney-Desmond, K. C., K. D. Bladon, and U. Silins. 2020. "Runoff and Sediment Production From Harvested Hillslopes and the Riparian Area During High Intensity Rainfall Events." *Journal of Hydrology* 582: 124452. https://doi.org/10.1016/j.jhydrol.2019.124452.

Reid, L. M., and T. Dunne. 1996. *Rapid Evaluation of Sediment Budgets*. Catena Verlag GMBH.

Riddle, B., J. Fox, B. Ford, A. Husic, and E. Pollock. 2025. "Fourteen-Year Fluvial Sediment Record Shows Non-Conservativeness of Organic

Tracers: Recommendations for Sediment Fingerprinting." *Hydrological Processes* 39, no. 1: e70054. https://doi.org/10.1002/hyp.70054.

Riddle, B., J. Fox, D. T. Mahoney, et al. 2022. "Considerations on the Use of Carbon and Nitrogen Isotopic Ratios for Sediment Fingerprinting." *Science of the Total Environment* 817: 152640. https://doi.org/10.1016/j.scitotenv.2021.152640.

Rossi, C. Q., M. G. Pereira, A. Loss, P. R. Gazolla, A. Perin, and L. H. C. dos Anjos. 2013. "Changes in Soil C and N Distribution Assessed by Natural $\delta^{13}C$ and $\delta^{15}N$ Abundance in a Chronosequence of Sugarcane Crops Managed With Pre-Harvest Burning in a Cerrado Area of Goiás, Brazil." *Agriculture, Ecosystems and Environment* 170: 36–44. https://doi.org/10.1016/j.agee.2013.03.008.

Rowntree, K. M., B. W. van der Waal, and S. Pulley. 2017. "Magnetic Susceptibility as a Simple Tracer for Fluvial Sediment Source Ascription During Storm Events." *Journal of Environmental Management* 194: 54–62. https://doi.org/10.1016/j.jenvman.2016.11.022.

Santos, A. M., J. D. Galvíncio, and M. S. B. de Moura. 2009. Desenvolvimento de Modelo de Balanço Hídrico Para Bacia Hidrográfica do rio Goiana-PE.

Skadell, L. E., F. Schneider, S. L. Bauke, W. Amelung, and A. Don. 2025. "Long-Term Management Effects on Depth Gradients of ^{13}C, ^{15}N and C/N Ratio in Agricultural Soils." *Geoderma* 458: 117341. https://doi.org/10.1016/j.geoderma.2025.117341.

Smith, H. G., and W. H. Blake. 2014. "Sediment Fingerprinting in Agricultural Catchments: A Critical Re-Examination of Source Discrimination and Data Corrections." *Geomorphology* 204: 177–191. https://doi.org/10.1016/j.geomorph.2013.08.003.

Stewart, H. A., A. Massoudieh, and A. Gellis. 2015. "Sediment Source Apportionment in Laurel Hill Creek, PA, Using Bayesian Chemical Mass Balance and Isotope Fingerprinting." *Hydrological Processes* 29, no. 11: 2545–2560. https://doi.org/10.1002/hyp.10364.

Stock, B., and B. Semmens. 2016. "MixSIAR GUI User Manual v3.1." https://doi.org/10.5281/zenodo.47719.

Upadhayay, H. R., S. Bodé, M. Griepentrog, et al. 2017. "Methodological Perspectives on the Application of Compound-Specific Stable Isotope Fingerprinting for Sediment Source Apportionment." *Journal of Soils and Sediments* 17: 1537–1553. https://doi.org/10.1007/s11368-017-1706-4.

Supporting Information

Additional supporting information can be found online in the Supporting Information section. **Table S1:** Kruskal–Wallis *H*-test results for the ability of each tracer to discriminate between the sediment sources. **Figure S1:** LDA scatter plots for the selected tracer sets for the $<63\,\mu m$ (a) and $<32\,\mu m$ (b) fractions. Shaded ellipsoids encompass 50% of the group variability. sugarcane cultivation (SC), unpaved roads (UR), channel banks (CB). **Table S2:** Results of virtual mixture tests comparing known and predicted sediment source contributions using RMSE (root mean square error) and MAE (mean absolute error).